Promega

High-Throughput SARS-CoV-2 Antibody Detection with Automation Capabilities

Lumit™ Dx SARS-CoV-2 Immunoassay

Laboratories need efficient, sensitive and reliable IVD tests for detecting antibodies to SARS-CoV-2. By leveraging bioluminescent technology, the Lumit™ Dx SARS-CoV-2 Immunoassay is an IVD test designed to improve antibody detection of SARS-CoV-2 in serum or plasma samples. The assay provides laboratories with a scalable solution that eliminates time-consuming wash steps and simplifies the workflow, taking you from sample to answer in under 1 hour.

Scalable, No-Wash Workflow that is Easy to Automate

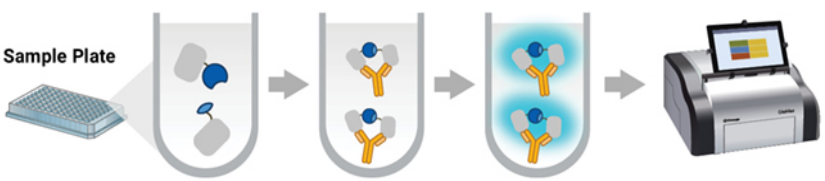

Add Lumit™ Dx CoV-2 LgBiT and Lumit™ Dx CoV-2 SmBiT to plate wells.

Add samples and controls to plate wells.

Incubate 30 minutes.

Add Lumit™ Dx Detection Reagent.

Incubate 3 minutes.

Measure luminescence.

Total assay time:

<60 minutes

Our Automation Experts Are Here to Help

We can help you adapt the Lumit™ Dx SARS-CoV-2 Immunoassay for use on many liquid handlers with in-lab or remote assistance and support.

Learn More: **promega.com/AntibodyTest**

The Lumit™ Dx SARS-CoV-2 Immunoassay is a qualitative in vitro diagnostic test intended for the detection of antibodies to SARS-CoV-2 in serum or plasma, utilizing a novel, proprietary detection system.

The Lumit™ Dx SARS-CoV-2 Immunoassay is indicated in conjunction with clinical presentation and the results of other laboratory tests as an aid in identification of patients with recent or prior SARS-CoV-2 infection. Results from the test should not be used as the sole basis for diagnosis or to exclude SARS-CoV-2 infection. See clinical sensitivity data for days post symptom onset of positive results observed. Positive results will occur only after infection and are indicative of recent or prior infection. False positive results can occur due to cross-reactivity from pre-existing antibodies or other possible causes.

Laboratories within the United States and its territories are required to report all positive results to the appropriate public health authorities.

Testing is limited to laboratories certified under the Clinical Laboratory Improvement Amendments (CLIA) to perform high complexity tests.

For prescription use only. For in vitro diagnostic use only.

Reports to healthcare providers should include the following information: Negative results do not preclude acute SARS-CoV-2 infection. If acute infection is suspected, direct testing for SARS-CoV-2 is necessary. Results from antibody testing should not be used to diagnose or exclude acute SARS-CoV-2 infection. Positive results may be due to past or present infection with non-SARS-CoV-2 coronavirus strains, such as coronavirus HKU1, NL63, OC43, or 229E. This test should not be used for screening of donated blood.

This test has not been reviewed by the FDA.

Clinical & Experimental Immunology
The Journal of Translational Immunology

Clinical and Experimental Immunology ORIGINAL ARTICLE doi:10.1111/cei.12124

The oxidative stress induced *in vivo* by Shiga toxin-2 contributes to the pathogenicity of haemolytic uraemic syndrome

S. A. Gomez,*[1] M. J. Abrey-Recalde,†[1] C. A. Panek,† N. F. Ferrarotti,‡ M. G. Repetto,‡ M. P. Mejías,† G. C. Fernández,† S. Vanzulli,§ M. A. Isturiz† and M. S. Palermo†

*Servicio de Antimicrobianos, Instituto Nacional de Enfermedades Infecciosas, ANLIS 'Dr Carlos G. Malbrán', †Laboratorio de Patogénesis e Inmunología de Procesos Infecciosos, Instituto de Medicina Experimental, (IMEX) (CONICET), ‡Laboratorio de Química General, Departamento de Química Analítica y Fisico- química, Facultad de Farmacia y Bioquímica, Universidad de Buenos Aires, and §División Patología, Instituto de Investigaciones Oncológicas, Academia Nacional de Medicina, Buenos Aires, Argentina

Accepted for publication 15 April 2013
Correspondence: M. S. Palermo, Instituto de Medicina Experimental (IMEX) (CONICET), Academia Nacional de Medicina, Pacheco de Melo 3081, C1425AUM Buenos Aires, Argentina.
E-mail: mspalermo@hematologia.anm.edu.ar

[1]These authors contributed equally to this paper.

Summary

Typical haemolytic uraemic syndrome (HUS) is caused by Shiga toxin (Stx)-producing *Escherichia coli* infections and is characterized by thrombotic microangiopathy that leads to haemolytic anaemia, thrombocytopenia and acute renal failure. Renal or neurological sequelae are consequences of irreversible tissue damage during the acute phase. Stx toxicity and the acute inflammatory response raised by the host determine the development of HUS. At present there is no specific therapy to control Stx damage. The pathogenic role of reactive oxygen species (ROS) on endothelial injury has been largely documented. In this study, we investigated the *in-vivo* effects of Stx on the oxidative balance and its contribution to the development of HUS in mice. In addition, we analysed the effect of anti-oxidant agents as therapeutic tools to counteract Stx toxicity. We demonstrated that Stx induced an oxidative imbalance, evidenced by renal glutathione depletion and increased lipid membrane peroxidation. The increased ROS production by neutrophils may be one of the major sources of oxidative stress during Stx intoxication. All these parameters were ameliorated by anti-oxidants reducing platelet activation, renal damage and increasing survival. To conclude, Stx generates a pro-oxidative state that contributes to kidney failure, and exogenous anti-oxidants could be beneficial to counteract this pathogenic pathway.

Keywords: haemolytic uraemic syndrome, oxidative stress, Shiga toxin 2

Introduction

The typical form of haemolytic uraemic syndrome (HUS) is caused by Shiga toxin (Stx)-producing *Escherichia coli* (STEC) infections [1]. It is usually preceded by bloody diarrhoea and is characterized by thrombotic microangiopathy that leads to haemolytic anaemia with red blood cell fragmentation, thrombocytopenia and acute renal failure [2]. In Argentina, HUS is the main cause of acute renal failure in the paediatric population, affecting between 10–15 children per 100 000 children aged below 5 years [3]. Systemic Stx toxaemia is considered to be central to the genesis of HUS by inducing damage to the vascular endothelial cells in the kidney, gastrointestinal tract and other organs and tissues [1]. However, Stx is not enough to cause the level of damage observed in renal biopses [4]. The endothelium suffers a marked shift towards a thrombotic status triggering platelet activation and aggregation, mainly as a consequence of Stx interaction with its specific receptor on endothelial cells [1]. The interaction of neutrophils and monocytes with activated endothelial cells contributes to the amplification of microvascular injury in the kidney [4,5].

Another factor that could contribute to the endothelial injury is the deleterious effect of oxidative stress. Aerobic cellular metabolism generates a physiological level of free radicals and oxidative stress that is removed or balanced by endogenous anti-oxidant compounds [6]. If free radical formation exceeds the anti-oxidant capacity, lipids, proteins and DNA may be oxidized. One of the main sources of free radicals and reactive oxygen species (ROS) are primed neutrophils through activation of the nicotinamide adenine dinucleotide phosphate–oxidase (NADPH) enzymes family [7]. Although 50–70% of neutrophil-produced ROS is restricted to the intracellular compartment, the other 30–50% is pulled through to the extracellular space,

promoting tissue damage [8,9]. The oxidative injury leads to alterations of membrane permeability, structure and cell function.

Conversely, glutathione (GSH) is the most important intracellular anti-oxidant that acts as a reducing agent and protects the cells sequestering ROS and detoxifying the intracellular medium [10]. GSH is the substrate of GSH peroxidase that reduces hydrogen peroxide (H_2O_2) or lipid peroxides (ROOH) generating oxidized glutathione (GSSG). Accumulation of GSSG is deleterious for the cell. Therefore, the increase in oxidative stress parallels the decrease in anti-oxidant capacity of the cell due to the loss of GSH [10,11].

During the course of the acute period, HUS patients have higher levels of lipid peroxidation of red blood cells [12], a rise in proteins with signs of an advanced oxidation process [13] and a higher concentration of GSSG than healthy controls [14]. In parallel, a significant decrease in superoxide dismutase (SOD) activity was found in erythrocytes from HUS patients, and the addition of their own plasma decreased SOD activity further [15]. Although, by injection of Stx alone, mouse models failed initially to recapitulate all features of HUS, this approach is often used to explore the direct effects of Shiga toxin intoxication on an animal [16]. In this regard, we have demonstrated previously that Stx type 2 (Stx2) injected in mice induces a significant increase in the respiratory burst and ROS basal production by polymorphonuclear leucocytes (PMN) [17]. Taken together, these data suggest that oxidative stress could be involved in tissue damage during HUS.

Because of the importance of restoring the oxidative balance, several compounds have been developed to be administered as exogenous sources of anti-oxidants to counteract the oxidative stress generated in different pathological conditions [18]. Among them, N-acetyl-L-cysteine (NAC) is a synthetic anti-oxidant derived from cysteine that acts by removing ROS and regulating several functions of the immune system [19]. NAC can act directly, by neutralizing ROS, or indirectly, by increasing GSH biosynthesis [20]. S-ethyl-L-cysteine (SEC) is the other cysteine-containing compound derived from garlic and acts by reducing thiol groups leading to anti-oxidant activity similar to NAC [21]. Therefore, using the HUS mouse model, the aim of this work was to study the *in-vivo* effects of Stx on the oxidative balance, and the protective capacity of synthetic anti-oxidants, by intravenous injection of purified Stx2.

Materials and methods

Reagents

SEC, NAC, dihydrorhodamine-123 (DHR-123), phorbol myristate acetate (PMA) and adenosine diphosphate (ADP) were obtained from Sigma (St Louis, MO, USA).

Mice

BALB/c mice were bred in the animal facility of Institute of Experimental Medicine (IMEX), Academia Nacional de Medicina, Buenos Aires. Male mice aged 9–16 weeks and weighing 20–25 g were used throughout the experiments. They were maintained under a 12-h light–dark cycle at 22 ± 2°C and fed with standard diet and water *ad libitum*. The experiments performed herein were approved by the Institutional Review Board for Animal Care.

PMN and platelet purification

Blood samples were obtained by puncture of the retro-orbital plexus at 24 and 72 h after Stx2 intoxication to obtain PMN and platelets, respectively. PMN were isolated from a pool of heparinized blood obtained from two to three mice. The cells were harvested by Ficoll-Hypaque separation followed by dextran sedimentation, as described previously [17].

For platelets, nine volumes of freshly drawn whole blood were collected into polyethylene tubes containing one volume of 3·8% (wt/vol) trisodium citrate solution in water. After half-diluting with HEPES-Mg buffer (pH 7·4), platelet-rich plasma (PRP) was obtained by centrifugation of whole blood at 100 ***g*** for 20 min at room temperature [22].

Flow cytometric studies

ROS generation. To determine the production of ROS by flow cytometry, DHR-123, a derivative of rhodamine 123, was used following the protocol described by Gomez *et al.* [17]. Briefly, isolated PMN (2×10^5) were incubated for 15 min at 37°C with 1 μM DHR-123. Subsequently, the cells were incubated with or without PMA 10 ng/ml for 15 min at 37°C 5% CO_2 in a humidified atmosphere. Immediately afterwards, the cells were washed and suspended in 0·3 μl of Isoflow (International Link, SA, Buenos Aires, Argentina). Green fluorescence was measured on 100 000 events with a Becton Dickinson (Franklin Lakes, NJ, USA) fluorescence activated cell sorter (FACScan) and analysed using the Cell-Quest program. PMN were identified and gated using forward-/side-scatter (FSC/SSC) dot-plot profiles and the fluorescence density was determined for cells within the neutrophil gate.

Evaluation of platelet fibrinogen binding. Platelet fibrinogen-binding assay was performed on PRP, as described previously [23]. Briefly, within 1 min, 10 μl of PRP was added to tubes containing 40 μl HEPES-Mg buffer (pH 7·4) and 2·5 μl of fluorescein isothiocyanate (FITC)

anti-fibrinogen antibody (1·2 g/l) (FITC-conjugated rabbit anti-human fibrinogen; Dako, Glostrup, Denmark) with or without 5 µl ADP (200 µmol/l). After mixing, the tubes were left for 10 min in the dark at room temperature without further agitation. The reaction was stopped by adding 50 µl 0·5% paraformaldehyde. Platelets were analysed using a Becton Dickinson FACScan. The platelet population was identified on the basis of its FSC/SSC profile, which distinguished it clearly from erythrocytes and white cells. The mean of green fluorescence intensity (MFI) of 10 000 platelets was analysed for each mouse with or without ADP-stimulation and represented as percentage increase for fibrinogen-binding capacity using the WinMDI program.

In-vivo treatments

Stx2 preparation. Stx2 was prepared as described previously [17]. Stx2 preparation was checked for endotoxin contamination by the Limulus amoebocyte lysate assay, given that 1 IU/ml is equal to 0·1 ng/ml of United States Pharmacopea standard *E. coli* lipopolysaccharide (LPS). The Stx2 preparation contained less than 100 pg LPS/µg of Shiga toxin protein. Stx2 was tested for cytotoxic activity on Vero cells, as described previously [17].

Stx2 treatment. Stx2 alone or in combination with LPS has been used with mouse models able to reproduce the features of human HUS [17,24,25]. We decided to inject intravenously (i.v.) purified Stx2 at doses of 2·5 ng/mice in the retro-orbital plexus, in the absence of additional LPS injection, in order to analyse the specific Stx2-dependent effects. The dose selected induced ≈ 90% mortality between 72 and 96 h after injection. The same batch and dose of Stx2 was used for all experiments.

Anti-oxidant treatment. We evaluated two protocols of intraperitoneal (i.p.) administration. In the first scheme, the anti-oxidants (NAC and SEC) were dissolved in saline solution and were administered daily beginning 48 h before Stx2 injection (*t*–48 h). In the second scheme, Stx2 was administered simultaneously with Stx2 (*t*0 h). In both cases, NAC and SEC were injected until the end of the experiment (250 mg/kg/day).

Urea studies

Biochemical determinations of urea in plasma were performed in an autoanalyser CCX Spectrum (Abbott Diagnostics Systems, Buenos Aires, Argentina) following standardized instructions. Values higher than the mean ± 2 standard deviations (s.d.) of age-matched normal mice was considered increased.

Determination of total GSH

For sample preparation, kidneys from euthanized mice were excised, rinsed and homogenized in $HClO_4$ 0·5 N (1 g organ in 50 ml acid). The homogenates were centrifuged at 5000 ***g*** for 10 min and the supernatants neutralized with Na_3 PO_4 0·44 M (1 ml supernatant in 0·5 ml Na_3PO_4).

For total GSH determination, the resultant supernatants (1 ml) were added to a reaction mixture composed of 1 ml phosphate buffer (0·1 M, pH7) and ethylenediamine tetraacetic acid (EDTA) 1 mM; 5-5′ di-tio-bis-nitrobenzoic acid (RSSR) 0·1 mM (in sodium and potassium phosphate buffer, pH 7); NADPH (4 mg/ml) in $NaCO_3$ 0·5% W/V and 6 U/ml of glutathione reductase. Absorbance was measured at 412 nm using oxidized glutathione (10 M) as standard. GSH concentration was calculated considering ε 412 nm = 13·5/mM/cm, and the result was expressed in µmol/g of organ [26].

Lipid peroxidation

Sample preparation. Kidneys from euthanized mice were excised rapidly, weighed and homogenized in a medium consisting of 120 mM KCl and 30 mM phosphate buffer, pH 7·4, at a ratio of 1 g liver/9 ml buffer at 0°C. The homogenates were centrifuged at 600 ***g*** for 10 min to discard nuclei and cell debris. The supernatant, a suspension of organelles and plasma membranes, was used as tissue homogenate [27].

Lipid peroxidation measurement. Lipid peroxidation was performed in kidney homogenates (pooled in pairs) as the level of malondealdehyde (MDA) by the reaction of thiobarbituric acid acid-reactive substances (TBARS), as described by Fraga *et al.* [28]. Kidney homogenates were deproteinized with 120 mM KCl, 30 mM phosphate buffer, pH 7·4, 4% w/v buthylhydroxytoluene in ethanol, 20% w/v thrichloroacetic acid and 0·7% w/v thiobarbituric acid. The deproteinized supernatant was heated at 100°C for 20 min, and the absorption of the solution was determined at 535 nm (ε = 1·5/mM/cm) and expressed as nmol MDA/g protein.

Histological studies

For histological studies both kidneys from each mouse were collected 72 h post-Stx2 or saline, or Stx2+NAC and Stx2+SEC (*t*–48 h only). Kidneys were bisected longitudinally, fixed in 10% neutral formalin and paraffin-embedded. The tissues were then stained with haematoxylin and eosin (H&E) and examined by light microscopy. A mean number of five sections of both kidneys from each mouse were examined for glomerular and tubular histological appearance and epithelial damage.

Table 1. Shiga toxin 2 (Stx2) effect on lipid peroxidation [malondealdehyde (MDA)] and total intracellular glutathione (GSH).

	MDA (nmol/mg of protein)	GSH (μmol/g of tissue)
Saline	74·5 ± 2·0 ($n = 8$)	3·6 ± 0·2 ($n = 8$)
Stx2	126·0 ± 9·5 ($n = 20$)*	1·5 ± 0·1($n = 20$)*

*$P < 0{\cdot}0001$ significantly different *versus* saline-treated mice.

Semi-quantitative renal tubular injury was evaluated by counting the number of damaged tubules per field according to the following criteria: swelling and cytoplasmic vacuolation, sloughing tubular epithelium, necrosis and apoptosis. All quantifications were performed by counting 10 non-overlapping cortical fields randomly at ×200 magnification from three mice per experimental group.

Statistical analysis

Survival and frequency data were analysed for significance using the χ^2 test. All other data correspond to the mean ± standard error of the mean (s.e.m.) of individual mice. Statistical differences were determined using the one-way analysis of variance (ANOVA). *A-posteriori* comparisons between two groups were performed using the Bonferroni test.

Results

Stx2 effect on lipid peroxidation and total intracellular GSH

To determine the level of oxidative stress induced by Stx2 in the kidney, we assayed the level of the most important product of lipid peroxidation, malondealdehyde (MDA), and total intracellular GSH content. As shown in Table 1, Stx2 injection increased MDA concentration significantly and reduced total GSH levels in whole kidney homogenates compared to saline treatment.

Protective effect of NAC and SEC on lipid peroxidation

To evaluate the effectiveness of exogenous anti-oxidants to counteract the level of lipid peroxidation induced by Stx2, we treated mice with two synthetic anti-oxidants, NAC and SEC, by daily administration of each drug under two different protocols: a long treatment, starting 48 h before Stx2 injection (*t*–48 h) (Fig. 1a), or a short treatment, simultaneous with the Stx2 injection (*t*0 h) (Fig. 1b). For both treatment schedules, anti-oxidants were continued until the end of the experiment. As shown in Fig. 1, NAC and SEC reduced MDA levels to basal values in Stx2-treated mice under both schedules (*t*0 or *t*–48 h). These results suggest that both anti-oxidant protocols were able to counterbalance the Stx2-enhancing effect on lipid peroxidation and cell membrane damage.

Effect of NAC and SEC on total GSH concentration

We studied whether the exogenous administration of anti-oxidants was able to restore GSH levels after the depletion induced by Stx2 in the kidney. Figure 2a,b shows that only SEC, and not NAC, was able to partially restore the GSH levels in mice treated with Stx2. In addition, treatment with NAC or SEC starting 48 h before Stx2 injection increased total GSH levels compared with saline-treated mice (Fig. 2a).

Effect of NAC and SEC on Stx2-induced mortality

We next evaluated the therapeutic potential effect of both anti-oxidants in survival rates after a lethal Stx2 dose. Both

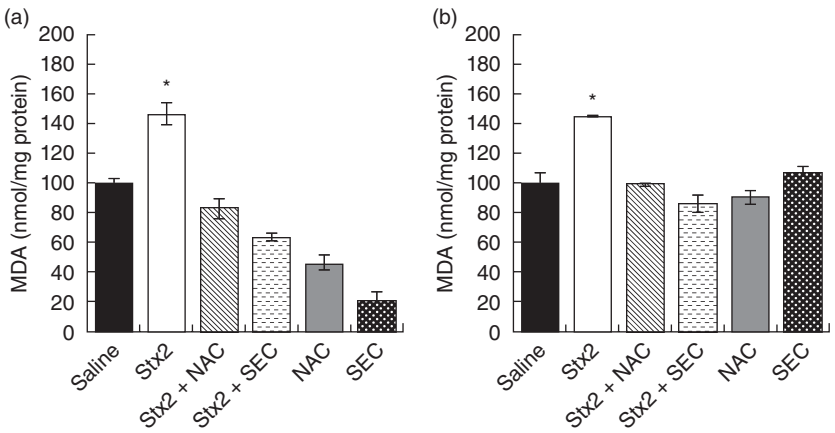

Fig. 1. N-acetyl-L-cysteine (NAC) and S-ethyl-L-cysteine (SEC) reduce lipid peroxidation in the kidney of mice treated with Shiga toxin 2 (Stx2). Kidney homogenates were treated as detailed in Methods. Bars show % increase of the mean ± standard error of the mean of two experiments ($n = 12$/group). (a) Treatment schedule with NAC or SEC started 48 h before Stx2 (*t*–48 h). Significant differences were found: *$P < 0{\cdot}001$ compared with all groups; (b) treatment with NAC or SEC started simultaneously with Stx2 (*t*0 h), *$P < 0{\cdot}001$ *versus* all groups. All comparisons by analysis of variance (ANOVA) multiple comparison test and posterior Bonferroni analysis.

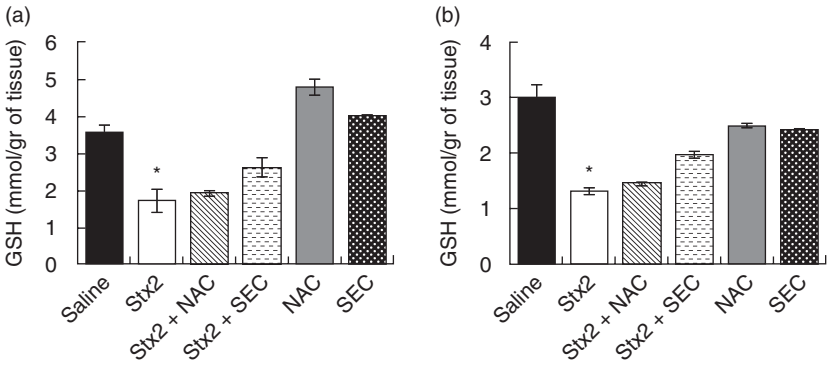

Fig. 2. N-acetyl-L-cysteine (NAC) and S-ethyl-L-cysteine (SEC) partially recover intracellular glutathione (GSH) concentration. Kidney homogenates were processed as explained in Methods. Each bar shows the mean ± standard error of the mean of two different experiments ($n = 20$/group pooled in pairs). (a) At *t*–48 h, significant differences were found: $^*P < 0{\cdot}05$ *versus* Shiga toxin 2 (Stx2)+SEC. (b) *t*0 h, $^*P < 0{\cdot}001$ *versus* saline and $P < 0{\cdot}01$ *versus* Stx2+SEC.

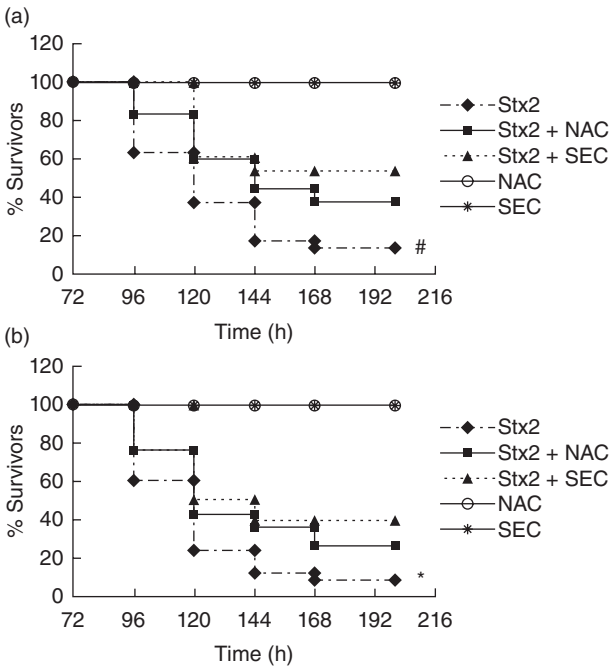

Fig. 3. N-acetyl-L-cysteine (NAC) and S-ethyl-L-cysteine (SEC) partially protect against Shiga toxin 2 (Stx2) mortality. Mice were treated with NAC or SEC starting 48 h before Stx2 (*t*–48 h) (a) or simultaneously (*t*0 h) (b). Survival was determined by frequent daily observations of the animals. The figures show the average percentage of survivors of at least three experiments ($n = 6$/group). $\#P < 0{\cdot}05$ *versus* Stx2+NAC and Stx2+SEC; $^*P < 0{\cdot}06$ *versus* Stx2+NAC and Stx2+SEC.

agents were able to reduce significantly the Stx2-induced mortality when given 48 h before Stx2 (Fig. 3a, *t*–48 h). When anti-oxidants were given simultaneously with Stx2, the survival rate was not significantly different from the Stx2 group (Fig. 3b, *t*0 h).

Effect of NAC and SEC on Stx2-induced renal damage

High plasma urea concentration correlates with renal damage [17]. Moreover, it provides a tool to follow-up the development of HUS in the murine model [17]. Therefore, animals were bled and urea concentration assayed 72 h post-Stx2 injection. NAC and SEC were able to reduce urea levels significantly in Stx2-injected mice (Fig. 4).

Histological study

To confirm that anti-oxidants improve mice survival upon Stx2 intoxication by inducing renal protection, kidneys were evaluated histologically at 72 h after Stx2 injection. Figure 5 shows representative sections of kidneys from mice treated with saline, Stx2 and Stx2+SEC (*t*–48 h protocol). Because the renal histological structures from mice treated with Stx2+NAC or Stx2+SEC under protocol *t*–48 h were similar, the figure shows only Stx2+SEC results. Mice given saline, NAC or SEC showed no damage (Fig. 5a, ii,iv). The kidneys from mice treated with Stx2 showed cortical necrotic foci, necrosis and loss of the general tubular and glomerular structure (Fig. 5a, i). In contrast, sections from mice treated with Stx2+SEC (Fig. 5a, iii) showed interstitial congestion

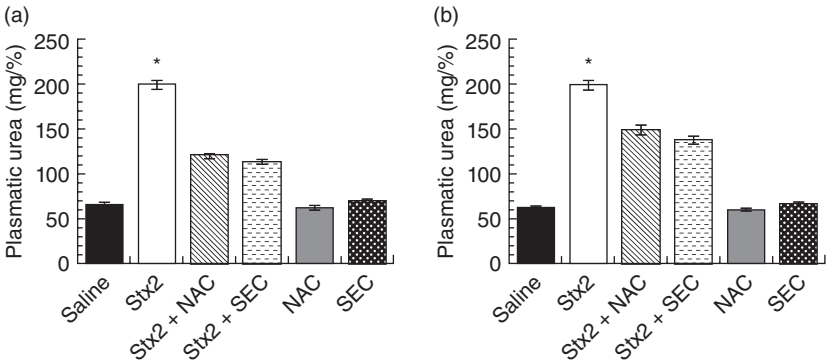

Fig. 4. N-acetyl-L-cysteine (NAC) and S-ethyl-L-cysteine (SEC) protect against Shiga toxin 2 (Stx2)-induced renal dysfunction. Samples of peripheral blood were obtained and processed to assay urea concentration, as explained in Methods. Bars show the mean ± standard error of the mean of four independent experiments ($n = 12$–22). (a) *t*–48 and (b) *t*0; significant differences were found for both protocols: $^*P < 0{\cdot}001$ *versus* all groups.

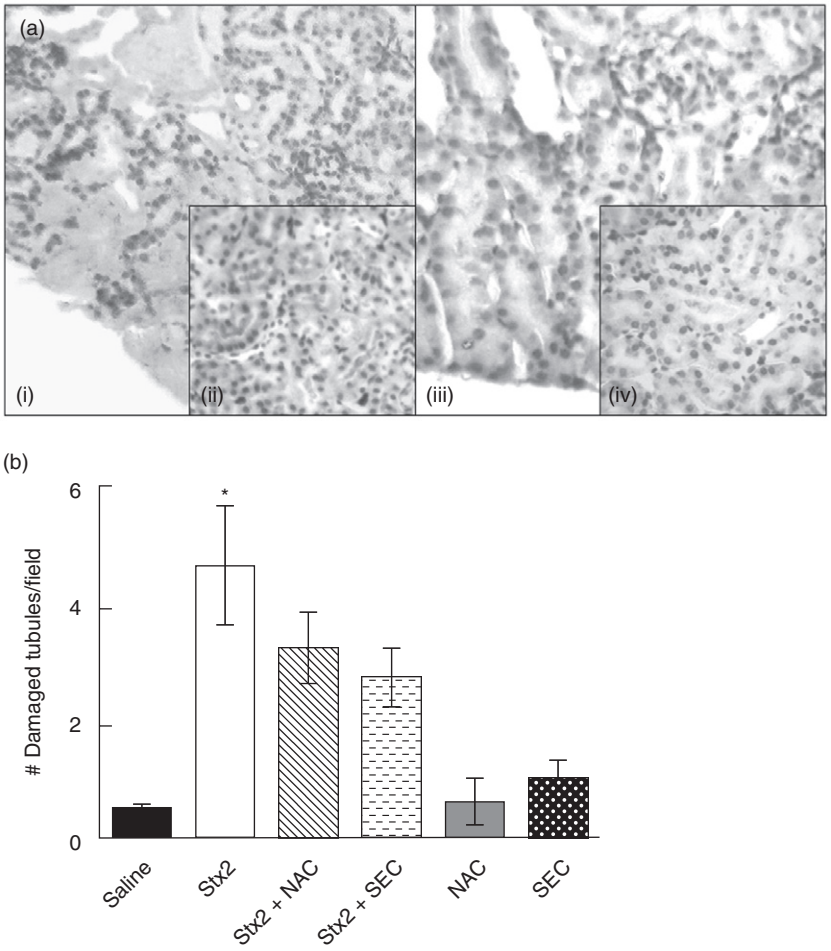

Fig. 5. Shiga toxin 2 (Stx2)-dependent injury in kidney tissue. Mice were treated with Stx2, S-ethyl-L-cysteine (SEC) or N-acetyl-L-cysteine (NAC) 48 h before Stx2 injection (Stx2+SEC, Stx2+NAC, *t*–48 h). Mice were euthanized 72 h after Stx2 injection and both kidneys were perfused with phosphate-buffered saline (PBS), excised, rinsed, fixed and stained as described in Methods. (a) Representative haematoxylin and eosin staining of paraffin kidney section fields from one mouse per experimental group. (i) Stx2, focal necrosis in the cortex region with loss of glomerular and tubular structure. The necrotic area is surrounded by conserved parenchyma. (ii) Insert: saline. Conserved parenchyma, glomerular and tubular structure. (iii) Stx2+SEC. Conserved structure with interstitial congestion. (iv) Insert, SEC. Conserved structure as in (ii). Magnification ×200. (b) Semiquantitative scoring of tubular damage. Number of damaged tubules in 10 cortical fields in control (saline) and treated mice. $^*P < 0{\cdot}001$ compared to saline and $P < 0{\cdot}05$ compared to Stx2+SEC or Stx2+NAC. All comparisons by analysis of variance (ANOVA) multiple comparison test and posterior Bonferroni analysis.

and conserved general structure with absence of necrotic foci. Coincident with the level of Gb3 expression in the mouse kidney, the Stx2 affects tubular epithelial cells preferentially [2]. Thus, we analysed comprehensively the renal tubule structure. Figure 5b shows that Stx2-treated mice presented a greater number of damaged tubules compared to Stx2+NAC- or Stx2+SEC-treated mice with the *t*–48 h protocol. The treatment under protocol *t*0 h with both anti-oxidants was less efficient, as we found no significant differences between the Stx2- and Stx2+SEC/Stx2+NAC-treated groups (data not shown).

Effect of NAC and SEC on cellular activation profile induced by Stx2

ROS production by PMN. Because treatment with anti-oxidants from 48 h before Stx2 reduced tissue damage and mortality rates significantly, we analysed further the effects of this treatment on the activation profile of the key cellular populations affected during HUS: neutrophils (PMN) and platelets. Confirming previous results [17], circulating PMN from Stx2-treated mice produce higher ROS than control mice in both conditions at baseline and upon *in-vitro* PMA stimulation. Figure 6 shows that both anti-oxidants administered from 48 h before Stx2 partially suppressed ROS production by PMN from Stx2-treated mice.

Platelet activation. Because platelets are sensitive to oxidative stress, we evaluated the activation status of platelets obtained from Stx2-intoxicated mice, with or without anti-oxidant treatment. Platelets obtained from Stx2-intoxicated mice at 72 h showed a slight increase in the level of membrane-bound fibrinogen (basal level, data not shown) but, most significantly, after *in-vitro* ADP stimulation they showed a lower increase in binding capacity (Fig. 7a). This phenomenon has been described in humans and HUS mouse models as 'exhausted' platelets [22,29]. NAC and SEC treatments commenced 48 h before Stx2 injection partially restored the level of response to *in-vitro* stimulation (Fig. 7b).

Discussion

The imbalance of anti-oxidants and ROS contribute to endothelial damage and lead to different diseases, in particular cardiovascular disease and hypertension. However,

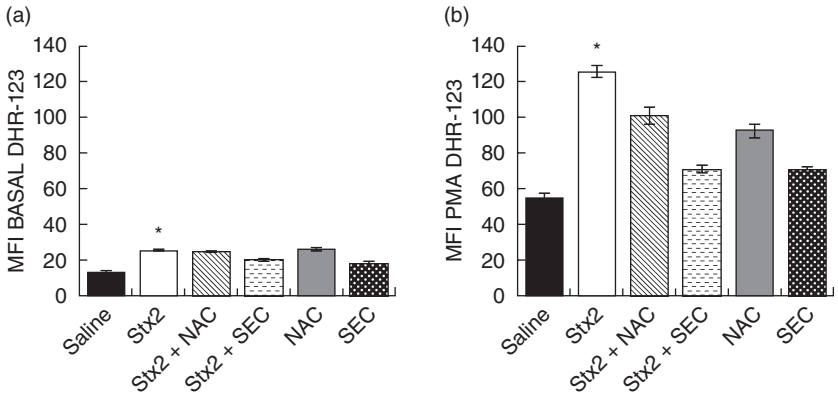

Fig. 6. N-acetyl-L-cysteine (NAC) and S-ethyl-L-cysteine (SEC) counteract the increase of reactive oxygen species (ROS) generation induced by Shiga toxin 2 (Stx2). NAC or SEC were administered 48 h before Stx2. Polymorphonuclear leucocytes (PMN) (2×10^5) were isolated from peripheral blood at 24 h after Stx2 injection and ROS production was measured by flow cytometry, as detailed in Methods. The figure shows the mean fluorescence intensity (MFI) of PMN from mice under different treatments in (a) basal conditions or (b) after phorbol myristate acetate (PMA) *in-vitro* stimulation. Each figure is a representative experiment showing the mean ± standard error of the mean of three mice per group (three repetitions). (a) *t*–48 h basal, **P* < 0·001 *versus* saline and *P* < 0·05 *versus* Stx2+SEC. (b) *t*–48 h PMA. **P* < 0·001 *versus* all groups.

a functionally compromised vascular endothelium is also associated with tissue-damaging responses, including inflammation, immune stimulation, oxidative stress and platelet activation/aggregation, as occurs during HUS [30]. Moreover, several lines of evidence support the hypothesis that ROS are crucially involved in the pathophysiology of renal failure [31], one of the central pathogenic events in HUS.

The major finding of this study was to demonstrate that Stx2 induces, directly or indirectly, a strong oxidative stress that participates in tissue damage and renal failure processes. Oxidative stress is seen both systemically and locally at the kidney level, through the enhancement of ROS production by circulating neutrophils and membrane lipid peroxidation in kidney, respectively. Although often referred to as a single entity, the term ROS actually comprises several factors that all potentially exert different vascular effects [32]. The superoxide anion (O_2^-) is central to ROS chemistry, because it may be converted into other physiologically relevant ROS (H_2O_2 and HO, in the presence of transition metals as Fe^{2+} and Cu^+) by enzymatic or non-enzymatic reactions. ROS derives from different sources, mainly neutrophils, endothelial cells and platelets. Notably, the magnitude of NAD(P)H-oxidase-derived O_2^- from endothelial cells and platelets are similar at the nanomolar range [33], but represents less than 1% of the amount of O_2^- released from activated neutrophils [34]. Therefore, enhanced ROS production by PMN may be the main source of oxidative stress during HUS. In fact, although PMN from HUS children on admission show impaired ROS production after direct protein kinase C stimulation [35], it has been suggested that they are low responders as a consequence of a previous activating process, which triggered the respiratory burst and the release of proteases associated with degranulation [4,35]. This process is similar to that found for platelets that circulate in a degranulated form as a consequence of a strong thrombotic stimulus prior to hospitalization [29,36].

The effect of ROS on cells and tissues are multiple and diverse. In particular, several independent studies have shown that ROS are prothrombotic, induce endothelial dysfunction and damage (lipid peroxidation), and O_2^- reduces the threshold for platelet activation to several stimuli [thrombin, collagen, ADP or arachidonic acid (AA)] and may even induce spontaneous aggregation [37]. Endothelial dysfunction or damage by oxidants are then associated with an enhanced risk for platelet activation. Increased platelet activity and thrombus formation would account for Stx-induced renal damage in patients with HUS. Stx and LPS have been proposed as factors that contribute to platelet activation in HUS [24,38]. In the present report we have demonstrated that oxidative stress induced by Stx2 is an additional activating stimulus for platelets, as anti-oxidant treatments improved platelet response after 72 h of Stx2 injection. ROS could activate platelets directly or indirectly by increasing their adhesion to the vascular endothelium. In this regard, an inflammatory response at the vessel wall induces the expression of adhesion molecules and the secretion of chemokines by vascular endothelial cells that may exacerbate the prothombotic status and favours platelet deposition [39,40].

It has been reported that O_2^- can react directly with GSH, resulting in a chain reaction that, ultimately, produces GSSG and additional O_2^-, shifting the intracellular redox balance to a lower GSH : GSSG ratio. In this regard, we also showed that the strong oxidative stress triggered by Stx2 intoxication exceeded endogenous anti-oxidant capacity, indicated by the GSH content in the kidney. Intracellular and extracellular GSH is not only the major non-protein anti-oxidant that protects the cell from oxidative stress; it

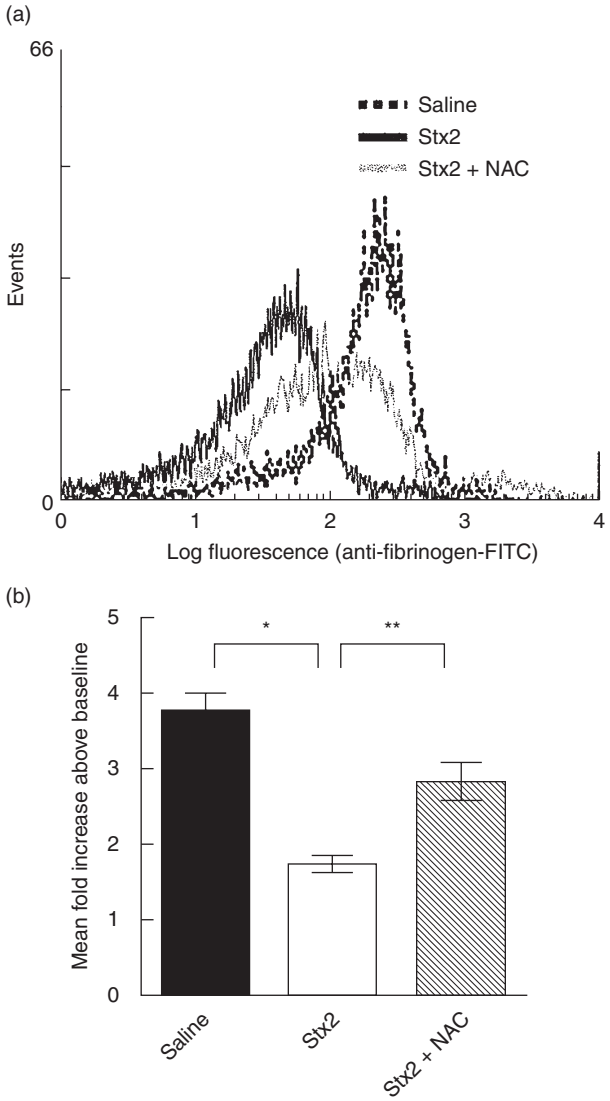

Fig. 7. N-acetyl-L-cysteine (NAC) partially restores platelet functionality. Adenosine diphosphate (ADP)-induced fibrinogen-binding sites *in vitro*. NAC was administered 48 h before Shiga toxin 2 (Stx2). Mice from different experimental groups were bled and euthanized at 72 h after Stx2. Platelets were stained with fluorescein isothiocyanate (FITC) anti-fibrinogen antibody, in the absence (basal) or presence of ADP (20 μmol/l) (stimulated) and analysed by flow cytometry, as described in Methods. (a) Representative histogram from one mouse of each experimental condition (saline, Stx2 and Stx2+NAC) showing fibrinogen binding after ADP stimulation. Basal levels were similar for all groups (data not shown). (b) Each bar represents the mean ± standard error of the mean of the mean fold-increase above the basal values for each experimental group ($n = 8$ mice/group). $^{*}P < 0{\cdot}0001$ and $^{**}P < 0{\cdot}01$. All comparisons by analysis of variance (ANOVA) multiple comparison test and posterior Bonferroni analysis.

also blocks ceramide generation, and thus the induction of apoptosis in human epithelial cells [41]. Taking into account that Stx induces apoptosis of renal tubular epithelial cells, as one of the specific effects upon interaction with its specific receptor, it would be interesting to investigate further whether the reduction of GSH in the kidney contributes to epithelial cell death during Stx intoxication. In addition, the reduction of GSH concentration has also been documented in the kidney during drug-induced nephrotoxicity processes [42]. Thus, extracellular supplementation of GSH or NAC is a known therapeutic approach to prevent oxidant-induced kidney injury. The mechanism of NAC action is controversial, because different effects have been documented under experimental conditions [43]. Among these effects, it has been described that NAC, being a precursor of GSH, restores its intracellular level, but also acts as a scavenger agent sequestering ROS [44,45] and ameliorates microcirculation by preventing angiotensin II- or nitric oxide-induced vasoconstriction [46].

In the mouse Stx2 intoxication model we found that both exogenous anti-oxidants, NAC and SEC, improved oxidative imbalance, reducing ROS production and lipid peroxidation, and protected mice partially against kidney failure and lethality. However, we observed that only SEC administration could restore the diminished levels of GSH after Stx2 intoxication, suggesting that, in this model, exogenous anti-oxidants could be acting mainly as ROS scavengers. In addition, Stx2 intoxication induces strong activation of the inflammatory response [2,25]. As HUS pathogenicity is complex and multi-factorial, it is difficult to alter the HUS evolution blocking only one of the pathogenic pathways.

Coincident with the strongest anti-oxidant effect, long preventive treatments (*t*–48 h) showed a more effective protective effect compared to shorter treatments (*t*0 h). These results are in accordance with previous reports indicating that only NAC pretreatment was effective in reducing the incidence and severity of acute kidney injury [43]. Taking into account that HUS develops several days after STEC infection [2], and considering that anti-oxidants are used widely with few documented adverse effects, anti-oxidant treatment should be started during the prodrome or diarrhoea phase to maintain oxidative–anti-oxidative balance and to prevent tissue damage.

As the extension of glomerular damage during the acute phase of HUS is the central defining event in the evolution of long-term renal dysfunction, in HUS-related research the search for therapeutic agents that allow control of the initial endothelial damage is mandatory.

Acknowledgements

This investigation was supported by Fundación 'Alberto J. Roemmers' (to CAP) and by Agencia Nacional de Promoción Científica y Tecnológica (PICT 417/08 and 427/11 to MSP), Argentina. The authors thank Héctor Costa and

Gabriela Camerano for assistance in mouse colony maintenance. They also thank Fundación de la Hemofilia and Academia Nacional de Medicina for the use of the FACScan flow cytometer.

Disclosure

All authors declare no competing interests.

References

1 Keir L, Coward RJ. Advances in our understanding of the pathogenesis of glomerular thrombotic microangiopathy. Pediatr Nephrol 2011; **26**:523–33.

2 Palermo MS, Exeni RA, Fernández GC. Interventions in hemolytic uremic syndrome (HUS), the major Shiga toxin-related complication in *E. coli* O157:H7 infections. Expert Rev Anti Infect Ther 2009; **7**:697–707.

3 Rivas M, Sosa-Estani S, Rangel J *et al*. Risk factors for sporadic Shiga toxin-producing *Escherichia coli* infections in children, Argentina. Emerg Infect Dis 2008; **14**:763–71.

4 Exeni RA, Fernandez GC, Palermo MS. Role of polymorphonuclear leukocytes in the pathophysiology of typical hemolytic uremic syndrome. Sci World J 2007; **7**:1155–64.

5 Zoja C, Buelli S, Morigi M. Shiga toxin-associated hemolytic uremic syndrome: pathophysiology of endothelial dysfunction. Pediatr Nephrol 2010; **25**:2231–40.

6 Freedman JE. Oxidative stress and platelets. Arterioscler Thromb Vasc Biol 2008; **28**:s11–16.

7 Karlsson A, Dahlgren C. Assembly and activation of the neutrophil NADPH oxidase in granule membranes. Antioxid Redox Signal 2002; **4**:49–60.

8 Li JM, Shah AM. ROS generation by nonphagocytic NADPH oxidase: potential relevance in diabetic nephropathy. J Am Soc Nephrol 2003; **14**:S221–6.

9 Brown GE, Stewart MQ, Bissonnette SA *et al*. Distinct ligand-dependent roles for p38 MAPK in priming and activation of the neutrophil NADPH oxidase. J Biol Chem 2004; **279**:27059–68.

10 Perricone C, De Carolis C, Perricone R. Glutathione: a key player in autoimmunity. Autoimmun Rev 2009; **8**:697–701.

11 Deneke SM, Fanburg BL. Regulation of cellular glutathione. Am J Physiol 1989; **257**:L163–73.

12 Ferraris V, Acquier A, Ferraris JR, Vallejo G, Paz C, Mendez CF. Oxidative stress status during the acute phase of haemolytic uraemic syndrome. Nephrol Dial Transplant 2011; **26**:858–64.

13 Aiassa V, Baronetti JL, Paez PL *et al*. Increased advanced oxidation of protein products and enhanced total antioxidant capacity in plasma by action of toxins of *Escherichia coli* STEC. Toxicol In Vitro 2011; **25**:426–31.

14 Li Volti S, Di Giacomo C, Garozzo R, Campisi A, Mollica F, Vanella A. Impaired antioxidant defense mechanisms in two children with hemolytic–uremic syndrome. Ren Fail 1993; **15**:523–8.

15 Dubey NK, Yadav P, Dutta AK, Kumar V, Ray GN, Batra S. Free oxygen radicals in acute renal failure. Indian Pediatr 2000; **37**:153–8.

16 Mohawk KL, O'Brien AD. Mouse models of *Escherichia coli* O157:H7 infection and Shiga toxin injection. J Biomed Biotechnol 2011; **2011**:258185. doi: 10.1155/2011/258185.

17 Gómez SA, Fernández GC, Camerano G *et al*. Endogenous glucocorticoids modulate neutrophil function in a murine model of haemolytic uraemic syndrome. Clin Exp Immunol 2005; **139**:65–73.

18 Millea PJ. N-acetylcysteine: multiple clinical applications. Am Fam Physician 2009; **80**:265–9.

19 Benrahmoune M, Therond P, Abedinzadeh Z. The reaction of superoxide radical with N-acetylcysteine. Free Radic Biol Med 2000; **29**:775–82.

20 Arfsten D, Johnson E, Thitoff A *et al*. Impact of 30-day oral dosing with N-acetyl-L-cysteine on Sprague–Dawley rat physiology. Int J Toxicol 2004; **23**:239–47.

21 Hsu CC, Huang CN, Hung YC, Yin MC. Five cysteine-containing compounds have antioxidative activity in Balb/cA mice. J Nutr 2004; **134**:149–52.

22 Dran GI, Fernández GC, Rubel CJ *et al*. Protective role of nitric oxide in mice with Shiga toxin-induced hemolytic uremic syndrome. Kidney Int 2002; **62**:1338–48.

23 Alves-Rosa F, Stanganelli C, Cabrera J *et al*. Rapid recovery of platelet count following administration of liposome-encapsulated clodronate in a mouse model of immune thrombocytopenia. Br J Haematol 2002; **116**:357–66.

24 Guessous F, Marcinkiewicz M, Polanowska-Grabowska R, Keepers TR, Obrig T, Gear AR. Shiga toxin 2 and lipopolysaccharide cause monocytic THP-1 cells to release factors which activate platelet function. Thromb Haemost 2005; **94**:1019–27.

25 Obrig TG, Karpman D. Shiga toxin pathogenesis: kidney complications and renal failure. Curr Top Microbiol Immunol 2012; **357**:105–36.

26 Akerboom TP, Sies H. Assay of glutathione, glutathione disulfide, and glutathione mixed disulfides in biological samples. Methods Enzymol 1981; **77**:373–82.

27 Repetto MG, Ossani G, Monserrat AJ, Boveris A. Oxidative damage: the biochemical mechanism of cellular injury and necrosis in choline deficiency. Exp Mol Pathol 2010; **88**:143–9.

28 Fraga CG, Leibovitz BE, Tappel AL. Lipid peroxidation measured as thiobarbituric acid-reactive substances in tissue slices: characterization and comparison with homogenates and microsomes. Free Radic Biol Med 1988; **4**:155–61.

29 Fong JS, Kaplan BS. Impairment of platelet aggregation in hemolytic uremic syndrome: evidence for platelet 'exhaustion'. Blood 1982; **60**:564–70.

30 Deshpande DD, Janero DR, Amiji MM. Therapeutic strategies for endothelial dysfunction. Exp Opin Biol Ther 2011; **11**: 1637–54.

31 Nath KA, Norby SM. Reactive oxygen species and acute renal failure. Am J Med 2000; **109**:665–78.

32 Wolin MS, Gupte SA, Oeckler RA. Superoxide in the vascular system. J Vasc Res 2002; **39**:191–207.

33 Krotz F, Sohn HY, Pohl U. Reactive oxygen species: players in the platelet game. Arterioscler Thromb Vasc Biol 2004; **24**:1988–96.

34 Lassegue B, Clempus RE. Vascular NAD(P)H oxidases: specific features, expression, and regulation. Am J Physiol Regul Integr Comp Physiol 2003; **285**:R277–97.

35 Fernandez GC, Gomez SA, Rubel CJ *et al*. Impaired neutrophils in children with the typical form of hemolytic uremic syndrome. Pediatr Nephrol 2005; **20**:1306–14.

36 Walters MD, Levin M, Smith C *et al*. Intravascular platelet activation in the hemolytic uremic syndrome. Kidney Int 1988; **33**:107–15.

37 Salvemini D, de Nucci G, Sneddon JM, Vane JR. Superoxide anions enhance platelet adhesion and aggregation. Br J Pharmacol 1989; **97**:1145–50.

38 Ghosh SA, Polanowska-Grabowska RK, Fujii J, Obrig T, Gear AR. Shiga toxin binds to activated platelets. J Thromb Haemost 2004; **2**:499–506.

39 Guo YL, Liu DQ, Bian Z, Zhang CY, Zen K. Down-regulation of platelet surface CD47 expression in *Escherichia coli* O157:H7 infection-induced thrombocytopenia. PLoS ONE 2009; **4**:e7131.

40 Weber C. Chemokines in atherosclerosis, thrombosis, and vascular biology. Arterioscler Thromb Vasc Biol 2008; **28**:1896. doi: 10.1161/ATVBAHA.108.177311.

41 Lavrentiadou SN, Chan C, Kawcak T *et al*. Ceramide-mediated apoptosis in lung epithelial cells is regulated by glutathione. Am J Respir Cell Mol Biol 2001; **25**:676–84.

42 Santos NA, Catão CS, Martins NM, Curti C, Bianchi ML, Santos AC. Cisplatin-induced nephrotoxicity is associated with oxidative stress, redox state unbalance, impairment of energetic metabolism and apoptosis in rat kidney mitochondria. Arch Toxicol 2007; **81**:495–504.

43 Wang HZ, Peng ZY, Wen XY, Rimmelé T, Bishop JV, Kellum JA. N-acetylcysteine is effective for prevention but not for treatment of folic acid-induced acute kidney injury in mice. Crit Care Med 2011; **39**:2487–94.

44 Heyman SN, Goldfarb M, Shina A, Karmeli F, Rosen S. N-acetylcysteine ameliorates renal microcirculation: studies in rats. Kidney Int 2003; **63**:634–41.

45 Aruoma OI, Halliwell B, Hoey BM, Butler J. The antioxidant action of N-acetylcysteine: its reaction with hydrogen peroxide, hydroxyl radical, superoxide, and hypochlorous acid. Free Radic Biol Med 1989; **6**:593–7.

46 Conesa EL, Valero F, Nadal JC *et al*. N-acetyl-L-cysteine improves renal medullary hypoperfusion in acute renal failure. Am J Physiol Regul Integr Comp Physiol 2001; **281**:R730–7.